ISSN: 0975-8585

Research Journal of Pharmaceutical, Biological and Chemical Sciences

A Fluorescence Quenching Study of the Human Serum Albumin-Quercetin Complex by Addition of Cd(II), Zn(II), and Co(II).

Udochukwu Okorafor and Rubén M Savizky*

Department of Chemistry, The Cooper Union for the Advancement of Science and Art, New York, NY 10003.

ABSTRACT

Fluorescence quenching studies were done on a human serum albumin-quercetin complex by adding three different divalent metal ions (Cd(II), Zn(II), and Co(II)) to form a tertiary complex. When quercetin binds to human serum albumin, two moieties of quercetin, QC1 and QC2, fluoresce after excitation at 295 and 450nm. The band shape of the QC1 emission peak was sensitive to temperature and the nature of the quencher. The band shape of the QC2 emission peak was sensitive to temperature only if tryptophan and tyrosine emissions were quenched. Cd(II) and Co(II) acted as quenchers for both QC1 and QC2. Zn(II) enhanced QC1 and QC2. Stern-Volmer plots were used to analyze the mechanisms for quenching QC1 and QC2. In the presence of Cd(II), a combination of static and collisional quenching was responsible for the quenching of QC1 and QC2. Collisional quenching was the dominant mechanism for QC1. For QC2, static quenching was the dominant mechanism for concentrations equal to and below 30 μM and collisional quenching was the dominant mechanism for concentrations above 30 μM. In the presence of Co(II), QC1 was quenched statically while QC2 was quenched both statically and collisionally, with static being the dominant quenching mechanism.

Keywords: Human serum albumin, quercetin, fluorescence quenching, Stern-Volmer

Corresponding author

ISSN: 0975-8585

INTRODUCTION

Human serum albumin (HSA) is the most abundant protein in human blood plasma and accounts for the majority of the antioxidant capacity of blood serum. HSA consists of 585 amino acids and its amino acids sequence has 17 disulfide bridges, one free thiol (Cys 34), and one tryptophan (Trp 214) [1]. Since HSA has tryptophan, it can florescence. Figure 1 shows the three-dimensional structure of HSA [2].

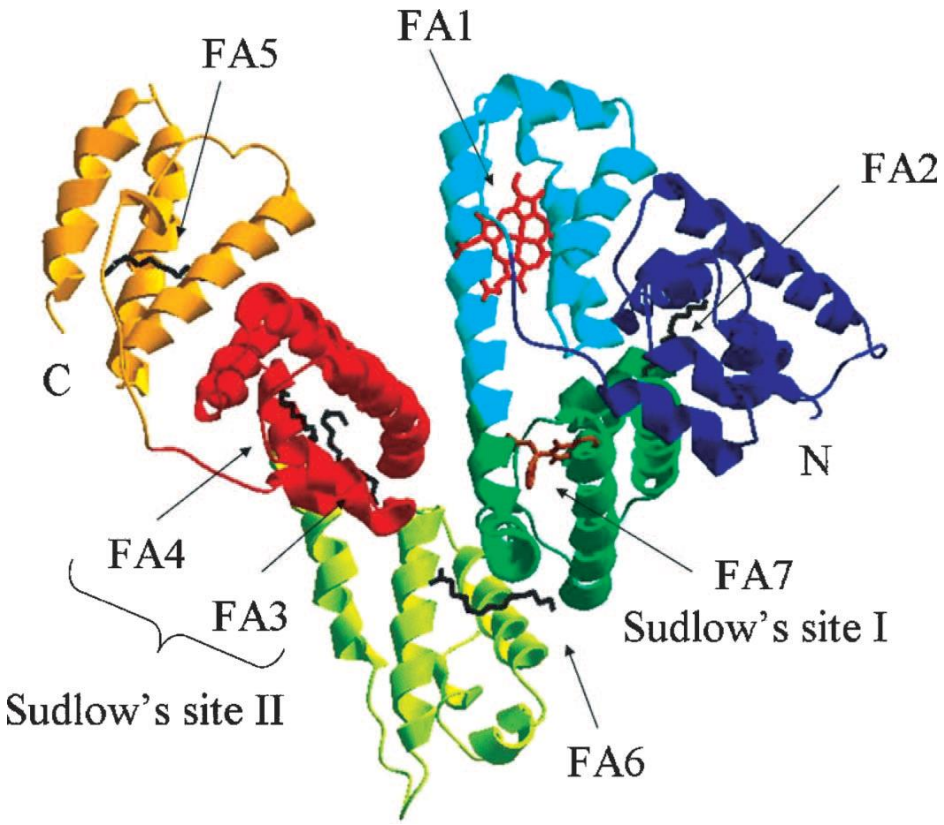

Figure 1: Crystal Structure Image for HSA [2]

HSA provides a depot for a wide variety of compounds including fatty acids, metal cations, and drug molecules because of its ability to bind ligands [2]. There are two ligand binding sites, named Site-I and Site-II [3]. These sites are labeled in Figure 1 as Sudlow sites in honor of the person who found them. Typically, bulky heterocyclic anions with their charges located in a fairly central position in the molecule bind to Site-I and aromatic neutral molecules bind to Site-II [4]. Metal cations bind to HSA at different binding sites. There are four binding locations for metals. The sites are the N terminus (NTS), the Cys34 residue, Metal Binding Site (MBS) /site A, and site B [5,6]. NTS is made of the first three residues of the albumin, Asp-Ala-His [6]. The Cys34 residue only allows binding of metal ions that can bind to HSA via a single metal-sulfur bond. Due to this restriction, neither Cd(II), Zn(II), nor Co(II) binds to Cys34. MBS consists of histidine-67, and 247, aspartic acid-249, and asparagine-99 [6]. The location of site-B has not been confirmed yet. The dissociation constants for metal ion binding to HSA are listed in Table 1 [6].

Table 1: Apparent dissociation constants for metal ion binding to HSA [6]

Metal Cation	NTS	MBS/site A	Site B
Cd(II)	Undetectable	3 µM	3 µM
Zn(II)	Undetectable	100 nM	~ µM
Co(II)	110 µM	90 µM	11 µM

As Table 1 shows, Cd(II) can bind to MBS and site B with equal affinity since the dissociation constants are the same. Zn(II) primarily binds to MBS with a dissociation constant for Zn(II) at MBS of 100 nM. Thus, Zn(II) binds more tightly to HSA than any of the other metal cations. For Co(II), MBS and site B are stronger

binding sites than NTS because both sites have lower dissociation constants for reversible metal ion binding to HSA. Site B is the preferred binding site for Co(II) since it has the lowest dissociation constant.

Quercetin, 2-(3,4-dihydroxyphenyl)-3,5,7-trihydroxy-4H-chromen-4-one, is a flavonoid that can bind to HSA. Flavonoids are polyphenols that are scaffolds made of two fused rings and one unfused ring [7]. They occur in nature and can be found in various fruits, nuts, vegetables, teas, and wine [8]. In humans, flavonoids can act as antioxidants, anti-inflammatory substances, and muscle relaxants [9]. Figure 2 shows the structure of which is classified as a flavonol, that is, aflavonoid that has substituted hydroxyl groups [10]. Previous research has shown that numerous flavonoids have intrinsic fluorescence and the hydroxyl group at the carbon 5 quenches intrinsic fluorescence [11]. Due to the numerous substituent groups, quercetin easily forms complexes with many metals [12].

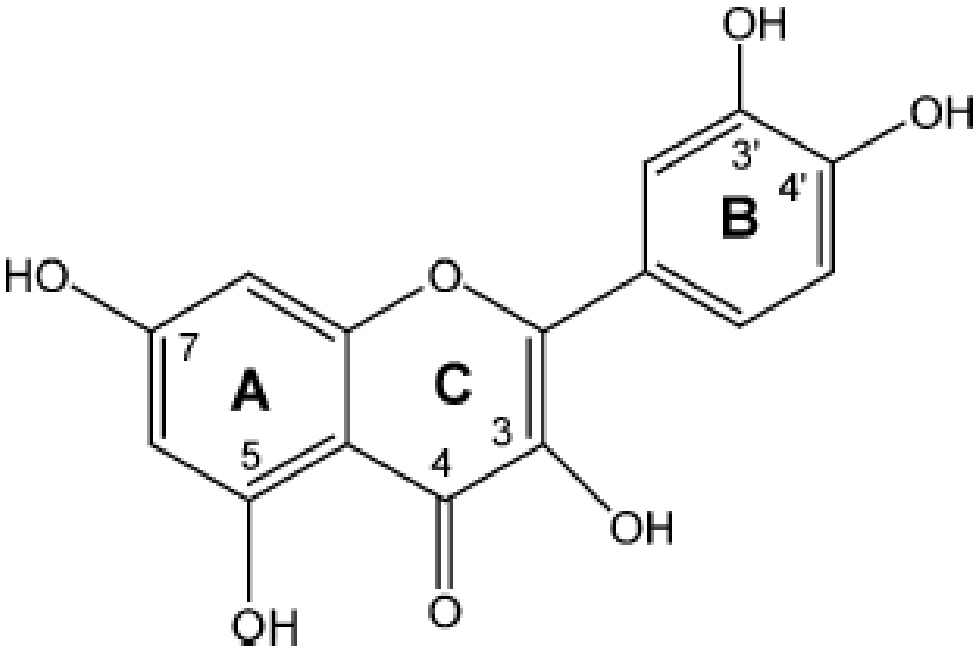

Figure 2: Structure of Quercetin [10]

When quercetin enters the bloodstream, it is carried by HSA [13]. Previous research has shown that quercetin binds to the large hydrophobic cavity, where tryptophan residues are located [11, 14]. When the HSA-quercetin complex is formed, two moieties, QC1 and QC2, of quercetin are created [4]. QC1 fluoresces after excitation at 295 nm, and QC2 fluoresces after excitation at 450 nm. The absorption spectra for QC1 with a maximum near 380 nm overlaps with the tryptophan emission spectrum with a maximum near 345 nm [4]. Previous research stated that the emission maximum of quercetin around 540 nm is due to resonance energy transfer between tryptophan-214 and quercetin [13].The band shape of QC1's emission peak is relatively sensitive to the nature of the quencher and the temperature [4]. According to Kim, temperature acts as a quencher for both QC1 and QC2 [4]. QC2's emission peak band shape is not sensitive to temperature but shifts if tryptophan or tyrosine emission was quenched [4].

Quenching is a decrease in intensity and can occur by various mechanisms. It can be used to study biochemical systems. Quenching studies can be used to understand the accessibility of a fluorophore because a decrease in intensity at a specific wavelength occurs when a quencher is added [4]. The two main quenching mechanisms are static and collisional. Both mechanisms occur only when a quencher is in contact with a fluorophore but have different methods in which they contact the fluorophore [15]. Static quenching is the quenching of a non-fluorescent ground-state complex between the fluorophore and the quencher. No emission of light occurs when the ground-state complex absorbs light because it immediately returns to the ground-state [15]. The scheme for static quenching is [4, 16]: $F+Q \overset{k_+[Q]/k_-}{\longleftrightarrow} F{:}Q$ .F is the fluorophore in its ground

state, and Q is the quencher.F: Q is the complex formed by the ground-state fluorophore and the quencher.k_+ is the second order binding constant, [Q] is the concentration of the quencher, and k_- is the first order dissociation rate constant of the F: Q complex.Collisional quenching is the deactivation of an excited fluorophore when the fluorophore is in contact with a quencher in solution [15]. Diffusion allows the quencher to be in contact with the fluorophore. This deactivation returns the fluorophore to its ground state. According to Mátyus, the scheme for collisional quenching for a simple case is [16]: $F+Q \overset{k_+[Q]/k_-}{\longleftrightarrow} F^*:Q \xrightarrow{k_q} F+Q$. F^* is the fluorophore in its excited state, k_- is the first order dissociation rate constant of the F^*: Q complex, k_q is the rate constant for quenching, and F^*: Q is the complex formed by the excited fluorophore and the quencher.

MATERIALS AND METHODS

All chemicals used in the experiment were analytical standard reagents. Albumin from human serum (lyophilized powder, ≥97% agarose gel electrophoresis), quercetin (≥95% (HLPC), solid), Trizma® hydrochloride (Tris-HCl) buffer solution (pH 7.4, 1M), methanol (99.8%, anhydrous), cadmium chloride (anhydrous, beads, ~10 mesh, 99.999% trace metals basis), zinc chloride (anhydrous, beads, amorphous,~10 mesh, 99.999% trace metals basis), and cobalt (II) chloride (anhydrous, beads, ~10 mesh, 99.999% trace metals basis) were purchased from Sigma Aldrich Co. Assurance Grade ASTM Type I Water Blank (AA Grade water) purchased from SPEX Certiprep was used throughout the experiment.

Fluorescence spectra were recorded by a Cary Eclipse Fluorescence Spectrophotometer usinga 1.00 cm quartz cell with a slit width of 5 nm. The "Zeroth order" option was selected as the emission wavelength for excitation experiments so that there is no set emission wavelength. Table 2 shows the settings for the emission spectra experiments.

Table 2: Fluorescence Spectrophotometer Settings

Spectra Type	Emission Spectra			
Excitation Wavelength (nm)	276	295	380	450
Start (nm)	280	300	480	460
Stop (nm)	400	575	580	600

The excitation filter and emission filter were set to be auto and open, respectively. The photomultipliers detector voltage was at 660 V. A water bath in conjunction with a single cell Peltier block was used for temperature dependent experiments. The selected temperatures were 30 °C and 36.5 °C. The Savitzky-Golay method was used to smooth the spectra with a factor of 5 and an interpolated factor of 5.

EXPERIMENTAL

A stock solution of HSA was made by placing 1 g of HSA into 25 mL of 50 mM Tris-HCl buffer solution. This stock solution of HSA was stored at -20 °C. A stock solution of 50 mM Tris-HCl was made by diluting 1 M Tris-HCl buffer solution with AA-Grade water. A 7.5 mM quercetin stock solution was made by mixing 0.0375 mmol of quercetin with 5 mL of methanol. The quercetin stock solution was stored in the dark at room temperature, specifically at the back of a drawer in the lab. 75 mM metal stock solutions were made by mixing 0.375 mmol of $CdCl_2$, $ZnCl_2$, and $CoCl_2$ with 5 mL of AA-Grade water on the day of the experiment. The metal stock solutions are then diluted to 7.5 mM before beginning experiments.

The polarity of the solvent, the structure of the fluorophore, and the interactions the fluorophore has with the solvent can cause a variety of effects on the fluorescence spectra, such as lowering the energy of the excited state fluorophore or shifting the emission maximum [15].The two solvents used are water and methanol, which are polar compounds. The maximum volume of the solvents when a metal ion solution was added four times was 20 µL for water and 5 µL for methanol. To test the effect of the solvents, a maximum of 20 µL of water and 20 µL of methanol were added to HSA.5 µL of a solvent, such as AA-Grade water or methanol, was added into 2.5 mL of 15 µM HSA.

To study the effect temperature has on the HSA-querceetin complex, 5 µL of 7.5 mM quercetin was added into 2.5 mL of 30 µM HSA. Each quercetin addition increased the quercetin concentration by 15 µM in the solution. Trials are run at 30 and 36.5 °C.

5 µL of 7.5 mM quercetin was added into 2.5 mL of 30 µM HSA. 5 µL of a 7.5 mM solution of a quencher, such as Cd(II), Zn(II), or Co(II) was added into the HSA-quercetin solution. Each quencher addition increased the quencher concentration by 15 µM in the solution. Trials are run at 30 and 36.5 °C. The time it takes to bring the HSA-quercetin solution to the desired temperature and the time it takes for the reaction of the quencher with the HSA-quercetin solution to occur must be accounted for before recording the excitation and emission spectra. The time ranged from 7 minutes to 15 minutes.

RESULTS AND DISCUSSION

The effect the cations had on the HSA-quercetin complex was studied. Each Cd(II) addition increased the concentration of Cd(II) by 15 µM when 5 µL of 7.5 mM Cd(II) solution was added to a mixture of 30 µM HSA and 15 µM quercetin. Changes in excitation around 285 nm in Figure 3a indicate that Cd(II) weakly affects the local environments around tyrosine and tryptophan residues. Furthermore, changes in excitation around 380 nm and 450 nm indicate that quercetin fluorescence is possibly affected by Cd(II) addition. The excitation spectrum in Figure 3b indicates that quercetin fluorescence is affected even more as temperature increases around 450 nm. Figure 3c shows that the peak from resonance energy transfer was quenched when Cd(II) is added. There is a slight red-shift when temperature is increased to 36.5 °C as shown in Figure 3d. The shift was negligible since it was barely noticeable in the band shape. The bands for each concentration are close to one another and overlap. Thus, a part of the change in peaks could be attributed to general noise. One possible reason why the 45 µM band and the 60 µM band overlap is the increase in concentration. As the concentration of quencher increases, it may take more time for the metal to bind to the HSA-quercetin complex. Since the reaction time for each trial was constant, there was no adjustment of reaction time for increased concentration. For an excitation of 295 nm and the addition of Cd(II) to a HSA-quercetin complex, the reaction time was 15 minutes for each addition of 15 µM of Cd(II). The emission spectra at an excitation wavelength of 380 nm should match the emission spectra at an excitation wavelength of 295 nm for the range of 490-575 nm. Figures 3e and 3f do not match the spectra of Figures 3c and 3d. This disagreement could possibly occur possibly because of noise in the system. Figure 3g shows that the peak caused by QC2 is quenched with the addition of Cd(II). As in Figure 3c and Figure 3d, the data corresponding to 45 and 60 µM overlaps in the excitation wavelength at 450 nm. There is a red shift in the emission maximum as Cd(II) is added for both temperatures (Figure 3g and Figure 3h). Increasing the temperature does not change the band shape of emission at excitation of 450 nm.

Next, the effect of Co(II) on the complex was investigated The emission spectra at an excitation of at 380 nm are not shown because changes in the spectra display the same trends as what was shown in the emission spectra at excitation at 295 nm with a range between 490 and 575 nm. Both tryptophan and tyrosine excitation decreased with increasing Co(II) concentration as shown in Figures 4a and 4b. Furthermore, changes in excitation around 380 nm and 450 nm indicate that quercetin fluorescence is affected by Co(II) addition. There is a red-band shift as Co(II) concentration increases. Upon addition of Co(II), both tyrosine and tryptophan residues slightly increased (Figures 4c and 4d). Thus, Co(II) possibly affects tyrosine and tryptophan residues. No band shift was observed in either figure. The addition of Co(II) quenched the tryptophan emission peak near 345 nm when the HSA-quercetin complex was excited at 295 nm (Figure 4e). There is no shift of the peak when Co(II) is added. There is no band shift when the temperature is increased (Figure 4f). The band shape stays the same even when temperature is increased. Figure 4g shows that the QC1 peak from resonance energy transfer was quenched when Co(II) is added. There is a slight red-shift when the temperature is increased to 36.5 °C, as shown in Figure 4h. The shift was negligible since it was barely noticeable in the band shape. When Co(II) concentration is 45 µM or 60 µM, the band shape changes. The same change in band shape occurs at those concentrations when the temperature is increased. One possible reason for the band shape change is that the peak is close to being completely quenched. Figure 6i shows that the peak cause by QC2 is quenched with the addition of Co(II). There is a red shift in the emission maximum as Co(II) is added for both temperatures (Figure 4i and Figure 4j). Increasing the temperature does not change the band shape of emission at excitation of 450 nm but quenches the peak.

Finally, the effects of Zn(II) were examined. Similar to what was observed with Co(II), the emission spectra at an excitation of 380 nm are not shown because the changes in the spectra display the same trends as what was shown in the emission spectra at excitation at 295 nm with a range between 490 and 575 nm. Changes in excitation around 285 nm for 30 and 36.5 °C in Figures 5a and 5b indicate that Zn(II) affects the local environments around tyrosine and tryptophan residues. Furthermore, changes in excitation around 380 nm and 450 nm indicate that quercetin fluorescence is affected by Zn(II) addition. The 60 µM band in Figure 5a varies from the other concentration bands because the spectrophotometer could not record intensities above 1000 a.u. Upon addition of Zn(II), both tyrosine and tryptophan residues slightly increased (Figures 5c and 5d). Thus, Zn(II) possibly affects tyrosine and tryptophan residues. No band shift was observed in either figure. Figure 5e shows that the peak from resonance energy transfer was enhanced when Zn(II) is added. There is no band shift when temperature is increased to 36.5 °C as shown in Figure 5f. Figure 5g shows that the peak for QC2 was enhanced when Zn(II) is added. There is red shift of the emission maximum as Zn(II) is added. When temperature is increased to 36.5 °C, there is a blue shift of the emission maximum, as shown in Figure 5h.

One effective method to study quenching is the Stern-Volmer (SV) equation. The Stern- Volmer equation can be written as [15]: $\frac{F_0}{F}=1+ k_{qc}\tau_0[Q]=1+ K_{SV}[Q]$where F_0 is the fluorescence intensity in the absence of quencher, F is the fluorescence intensity in the presence of quencher, k_{qc} is the bimolecular quenching constant; τ_0 is the lifetime of the fluorophore in the absence of quencher, and [Q] is the concentration of quencher. K_{SV} is the Stern-Volmer quenching constant and is equal to $k_{qc}\tau_0$. The Stern-Volmer equation is primarily used for collisional quenching but can also be used for static quenching.Applying the SV equation to a quenching study leads to plotting the relative fluorescence intensity versus the quencher concentration. Due to the SV equation, the y-intercept of the line should be at 1. A linear SV plot indicates that a fluorophore or a class of fluorophores is accessible to the quencher [15]. Linearity does not mean that collisional quenching has occurred since static quenching can also have a linear SV plot. If the SV plot has an upward curvature, concave towards the y-axis, then there is both collisional quenching and static quenching [15]. If the SV plot has a downward curvature then the quencher was unable to access a fraction of the fluorophores because of the location of the fluorophores [17].

Determining the type of quenching can be done by varying the temperature, varying the viscosity, or making lifetime measurements. Higher temperatures increase the diffusion rate of the quencher. Thus, more collisional quenching occurs and the SV plot moves closer to the x-axis. Higher temperatures also cause dissociation of the complexes since they are weakly bound. Thus, less static quenching occurs and the SV plot moves closer to the y-axis [15].The type of quenching occurring shows the complex that is formed by the fluorophore.

For Cd(II), both collisional and static quenching mechanisms are responsible for the decrease in the QC1 peak in Figure 6a since the SV plots clearly have a non-linear relationship. The average intensity of the range 530-533 nm for an excitation wavelength of 295 nm was used to find $\frac{F_0}{F}$ for both 30 and 36.5 °C. The range was chosen because the peaks of QC1 existed in that range for the varying concentrations. Collisional quenching is the dominant mechanism since the SV plot moves closer to the y-axis when temperature increases. The SV plots are concave down and indicate that QC1 is slightly shielded from Cd(II). Both collisional and static quenching are responsible for the decrease in the QC2 peak in Figure 6b since the SV plots clearly have a non-linear relationship. The average peak intensity from the range 527-533 nm for an excitation wavelength of 450 nm was used to find $\frac{F_0}{F}$ for both 30 and 36.5 °C. The SV plots are concave down and indicate that QC2 is slightly shielded from Cd(II). At low concentrations of Cd(II), the dominant quenching mechanism is possibly static quenching since $\frac{F_0}{F}$ increases upon increasing temperature. However, collisional quenching is dominant in solution having concentrations of Cd(II) that are greater than 30 µM.

Since Co(II) significantly shifts the emission maximum, the value of $\frac{F_0}{F}$ at 60 µM Co(II) was not included in order to find the SV relationship for the remaining range of Co(II) concentrations. At an excitation of 295 nm, a maximum emission by QC1 at different Co(II) concentrations was observed in the range of 525 nm-529 nm for 30 °C and in the range of 525-530 nm for 36.5 °C. The averages of the peak intensities in the ranges were used to calculate K_{SV} at 30 and 36.5 °C (Figure 6c and 6d). The K_{SV} values at 30 and 36.5 °C are 9.667×10^3 and 8.571×10^3 L/mole, respectively. Static quenching is most likely the dominant mechanism since the linearity moved toward the x-axis at higher temperature. The decrease in R^2 with a temperature increase

ISSN: 0975-8585

suggests that static quenching was not the only quenching mechanism but the other quenching mechanisms were minor. The SV plot for 30 °C is linear and thus static quenching is responsible for quenching QC1 at this temperature. Since the SV plot is not linear for 36.5 °C, there has to be both collisional and static quenching occurring at QC1 at this temperature. At an excitation of 450 nm, a maximum emission by QC2 at different Co(II) concentration were observed in the range 528 nm-532 nm for 30 °C and in the range 530-534 nm for 36.5 °C. The values of the range for 36.5 °C are larger than the values of the range for 30 °C due to the red shift that occurs when temperature increases. The averages of the intensities in the ranges were used to calculate K_{SV}at 30 and 36.5 °C. The K_{SV} values at 30 and 36.5 °C are 2.413×10^4 and 2.219×10^4 L/mole, respectively. Static quenching is most likely the dominant quenching mechanism since the linearity moved toward the x-axis at higher temperature. The small increase in R^2 with a temperature increase suggests that other quenching mechanisms occur at a slightly lower rate when temperature increases. Since the SV plots are not linear, there is both collisional and static quenching occurring at QC2.

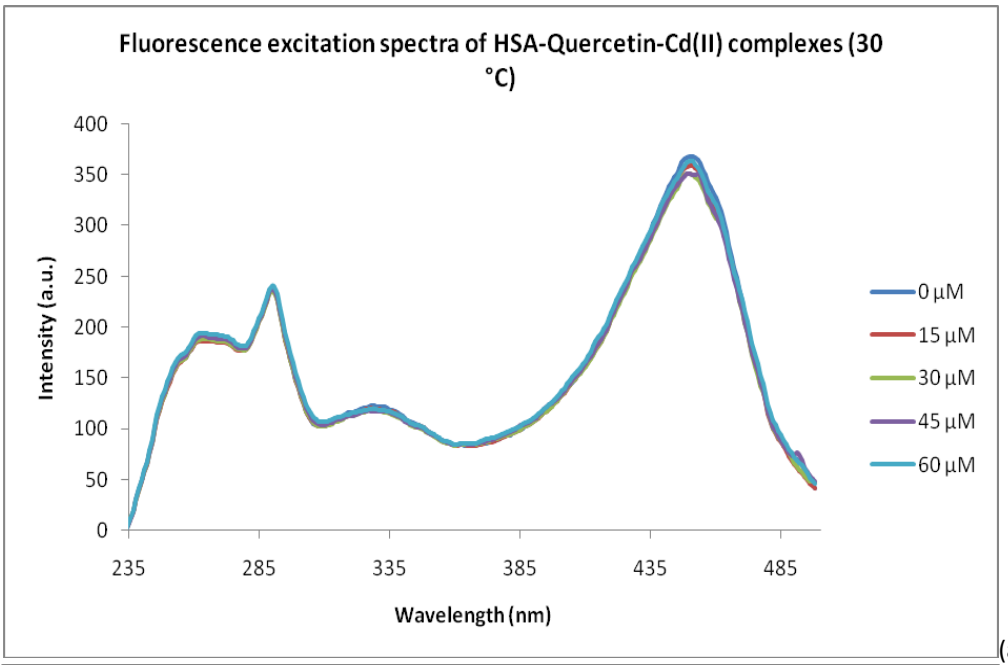

(a)

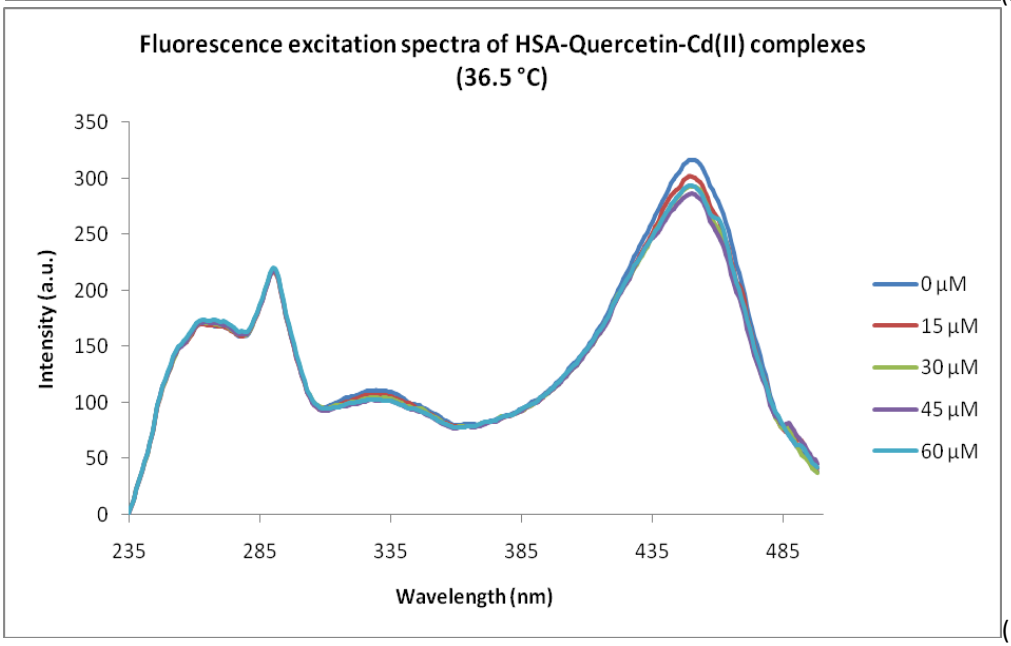

(b)

ISSN: 0975-8585

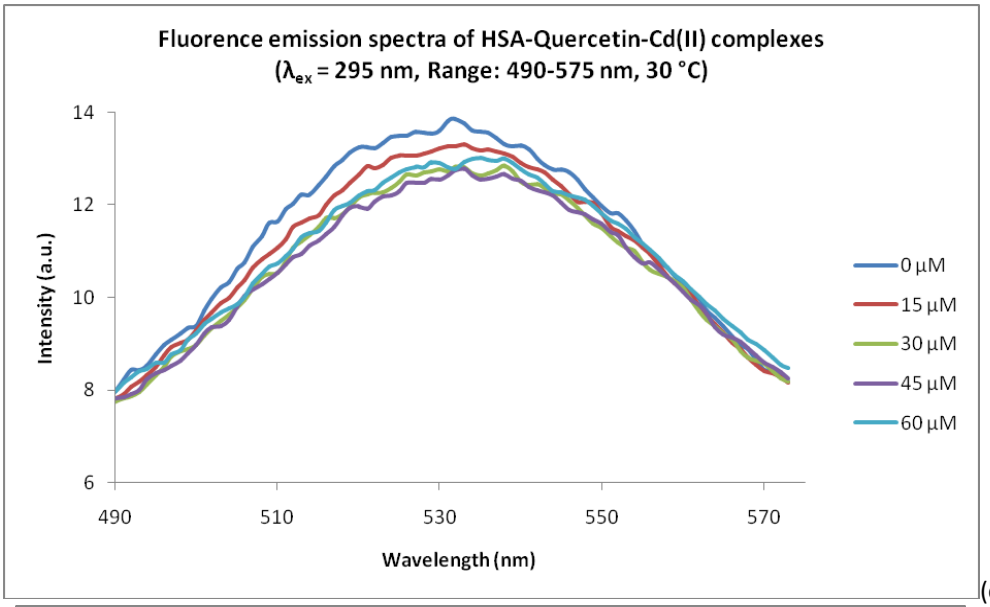

(c)

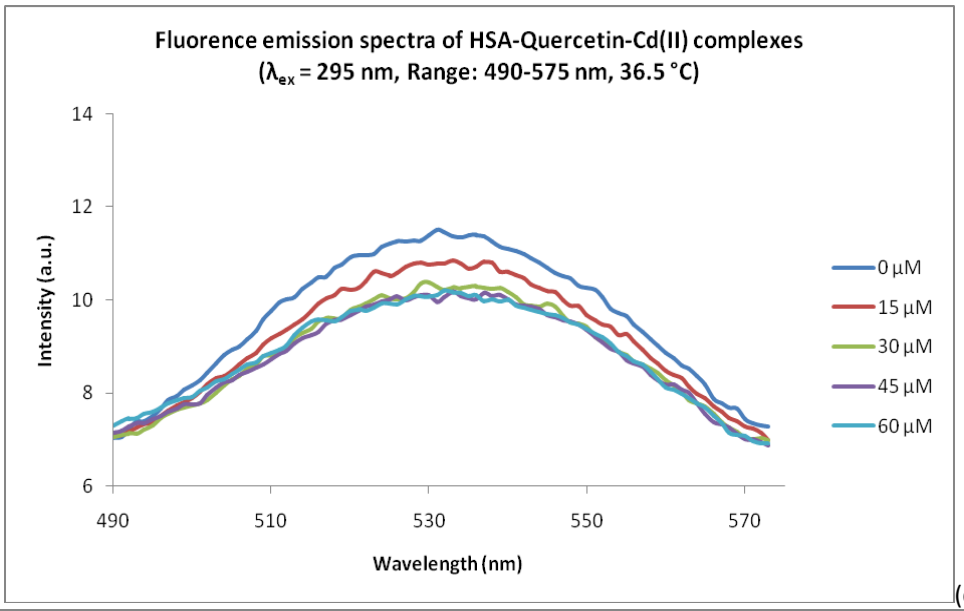

(d)

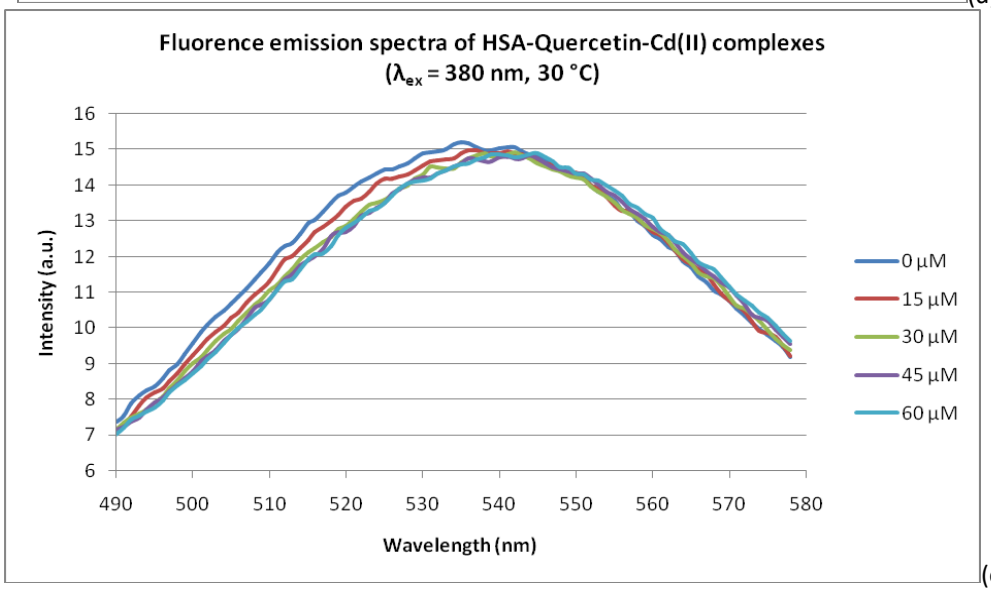

(e)

ISSN: 0975-8585

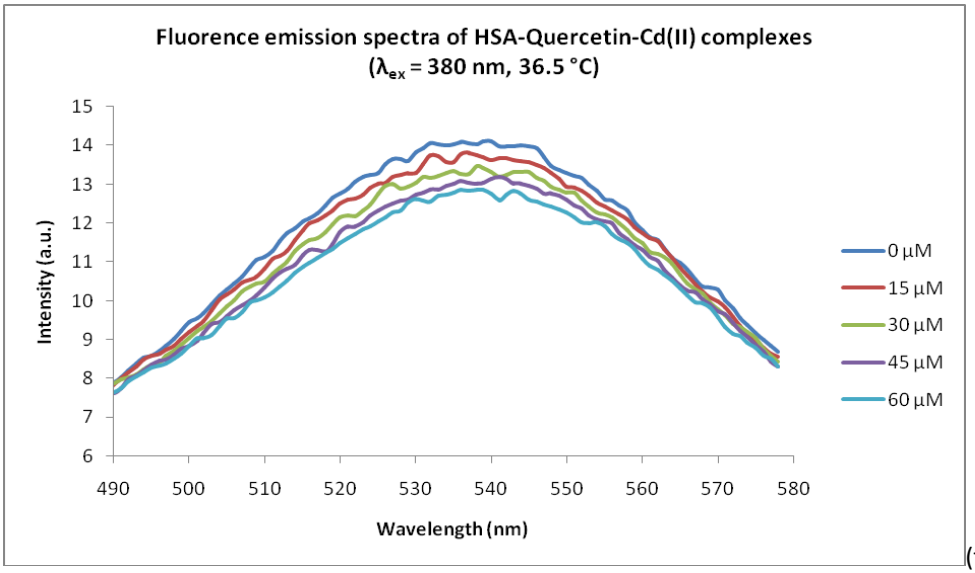

(f)

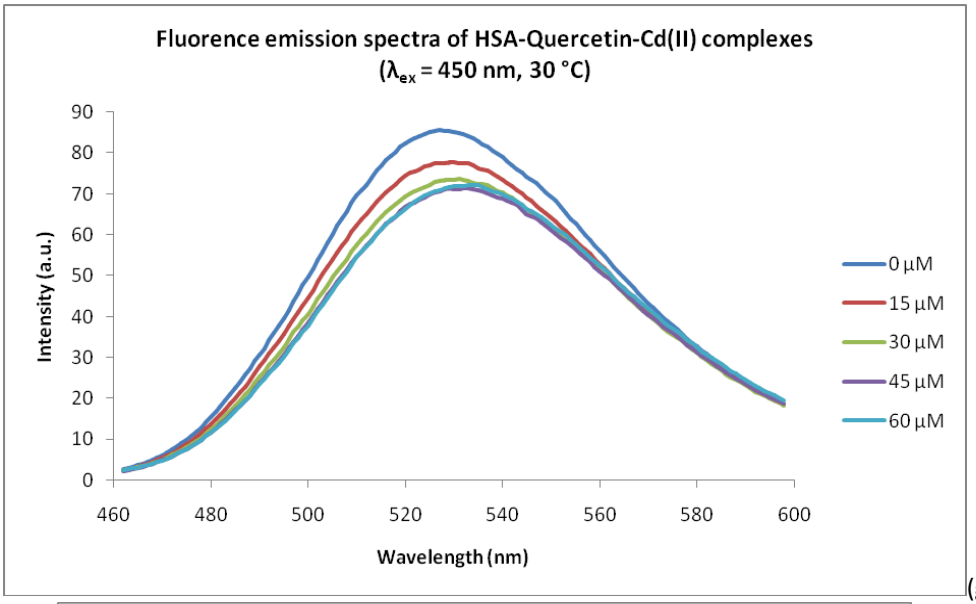

(g)

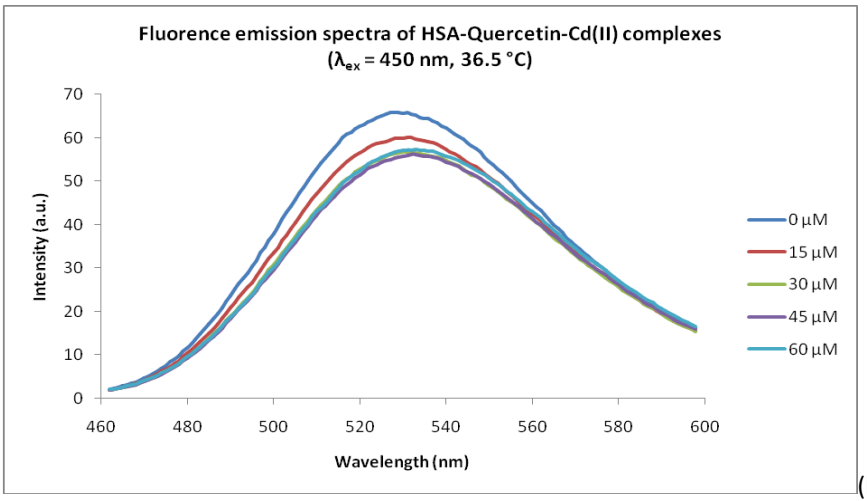

(h)

Figure 3: Fluorescence studies of HSA-quercetin-Cd(II) complexes. All experiments were performed using a scan rate of 120 nm/min. (a) and (b) Excitation spectra of solutions containing 30 µM HSA, 15 µM quercetin,and varying amounts of Cd(II) in 50 mMTris-HCl buffer at temperatures of 30 and 36.5 °C, respectively. (c) and (d) Emission spectra of the same solutions in (a), using an excitation wavelength of 295

ISSN: 0975-8585

nm at temperatures of 30 and 36.5 °C, respectively. (e)and (f) Emission spectra of the same solutions in (a), using an excitation wavelength of 380 nm at temperatures of 30 and 36.5 °C, respectively. (g) and (h) Emission spectra of the same solutions in (a), using an excitation wavelength of 450 nm at temperatures of 30 and 36.5 °C, respectively.

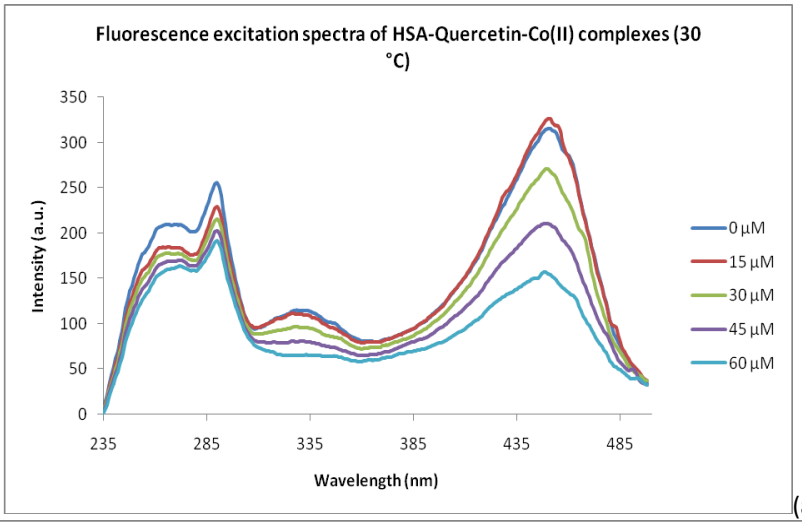

(a)

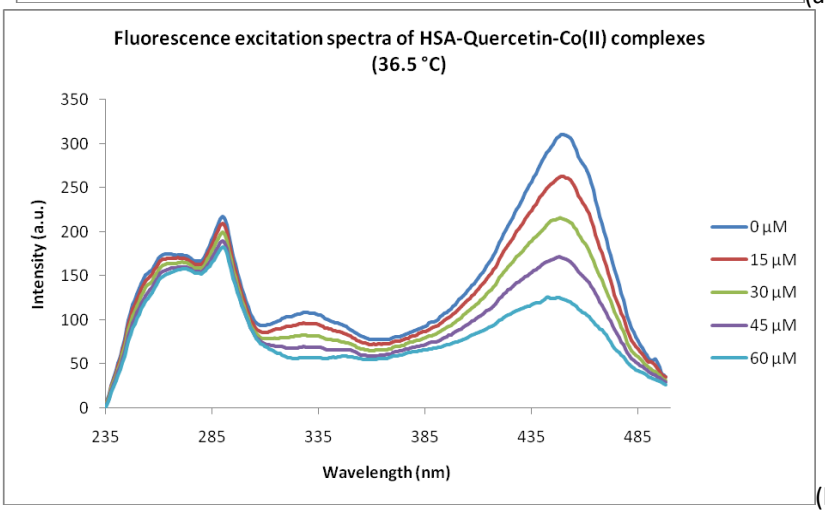

(b)

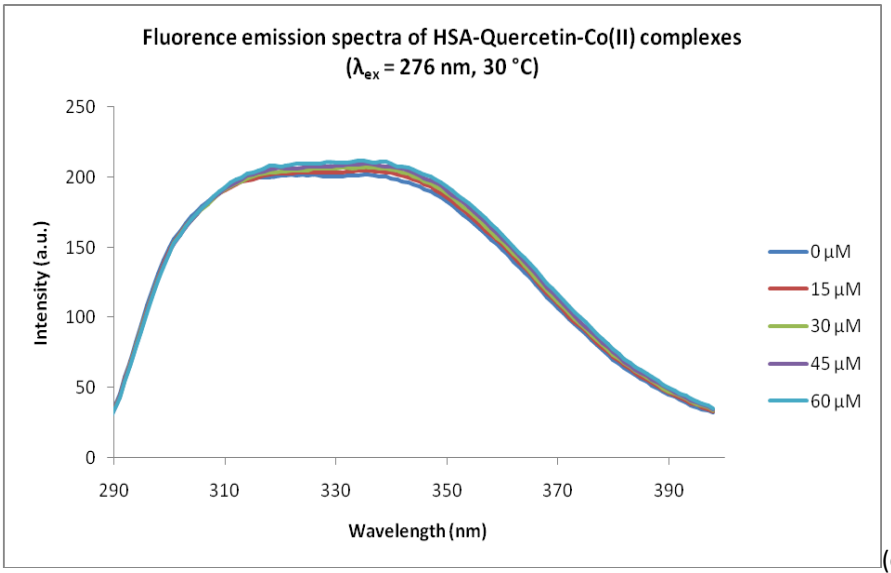

(c)

ISSN: 0975-8585

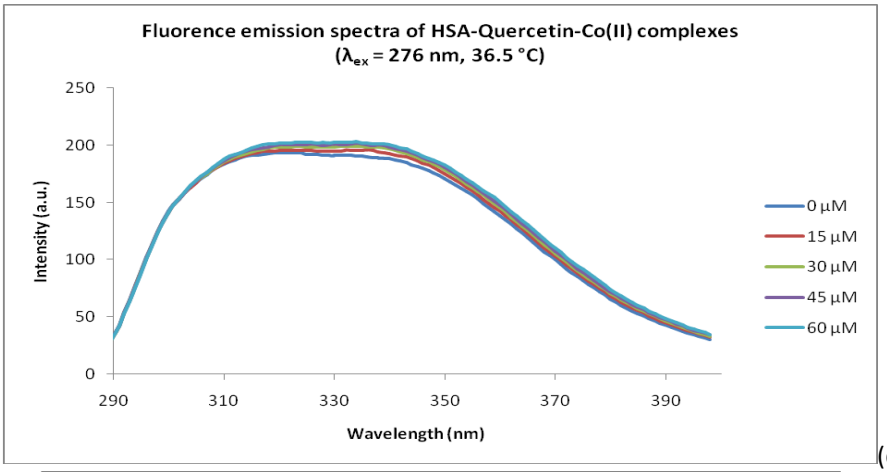

(d)

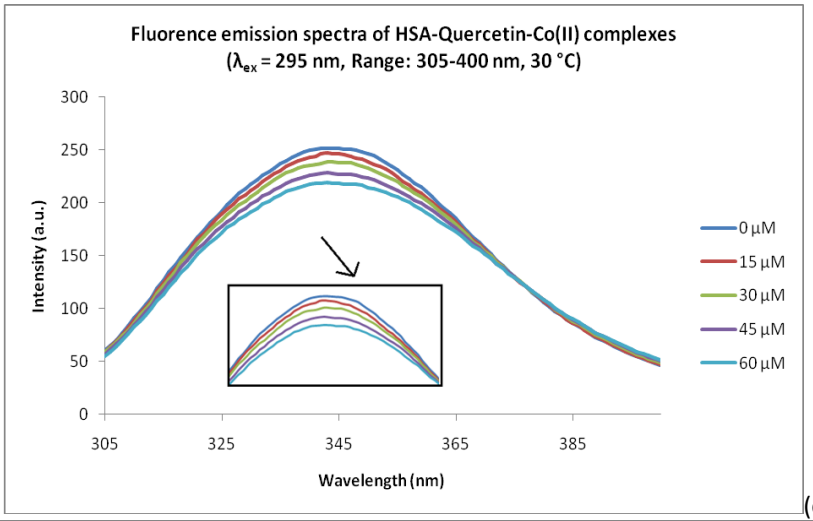

(e)

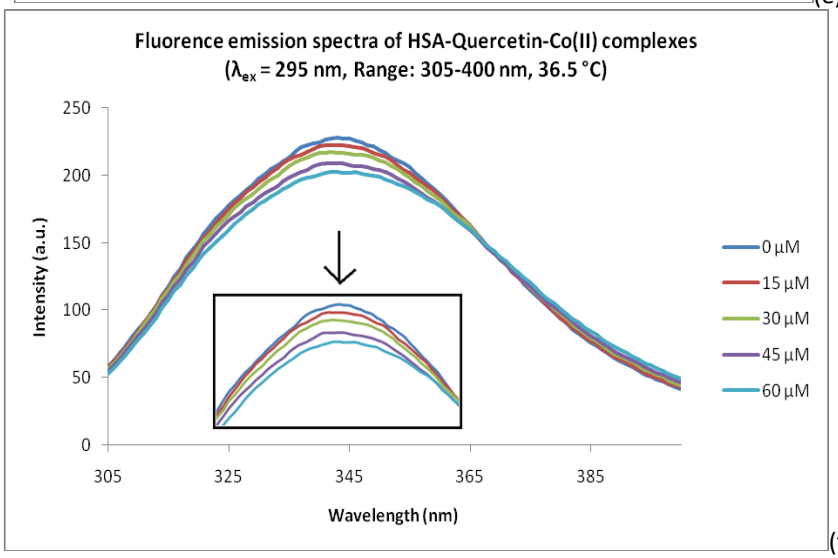

(f)

ISSN: 0975-8585

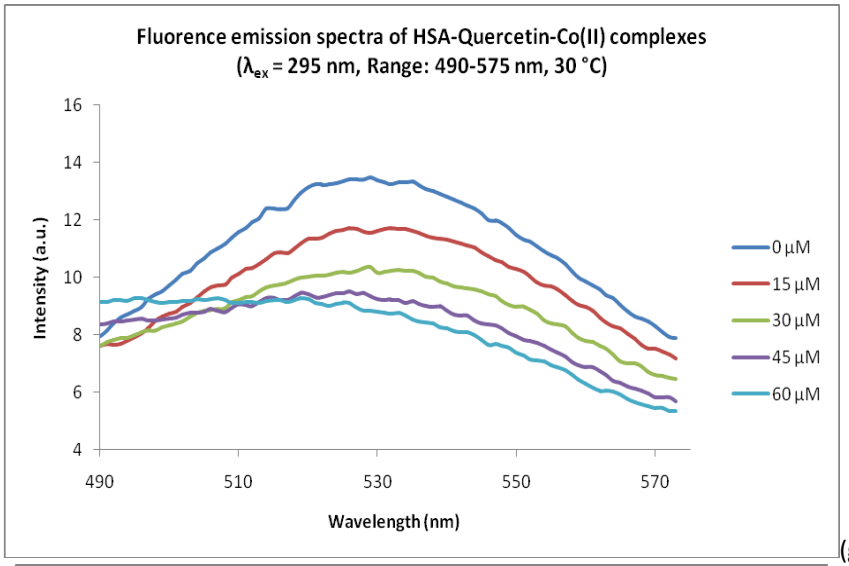

(g)

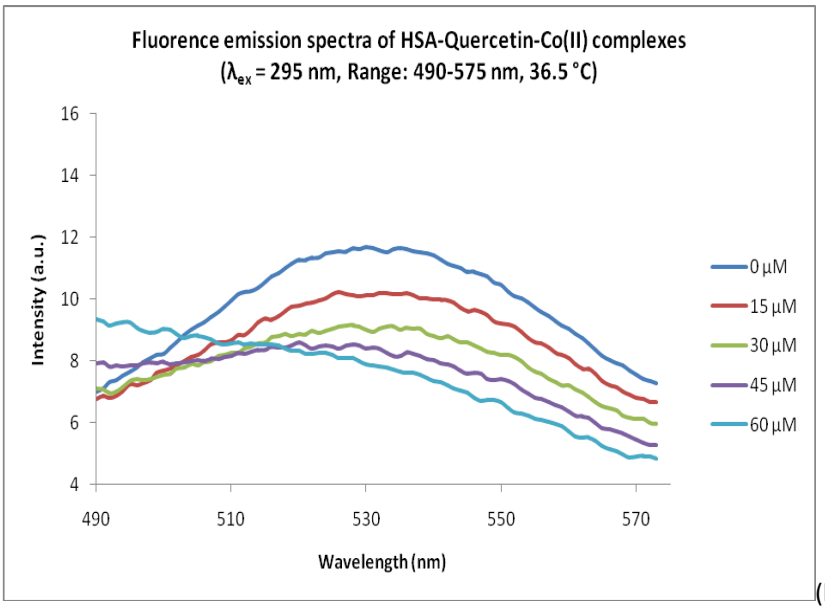

(h)

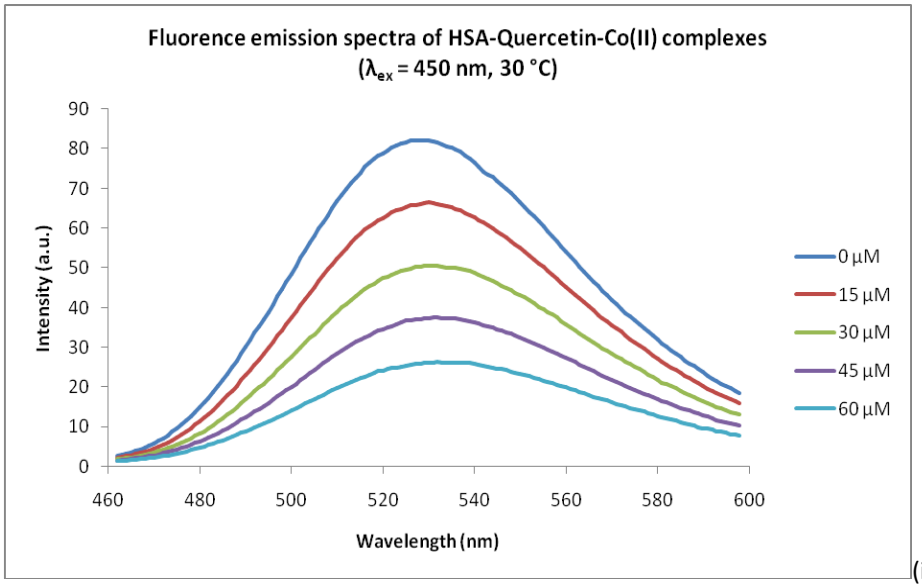

(i)

ISSN: 0975-8585

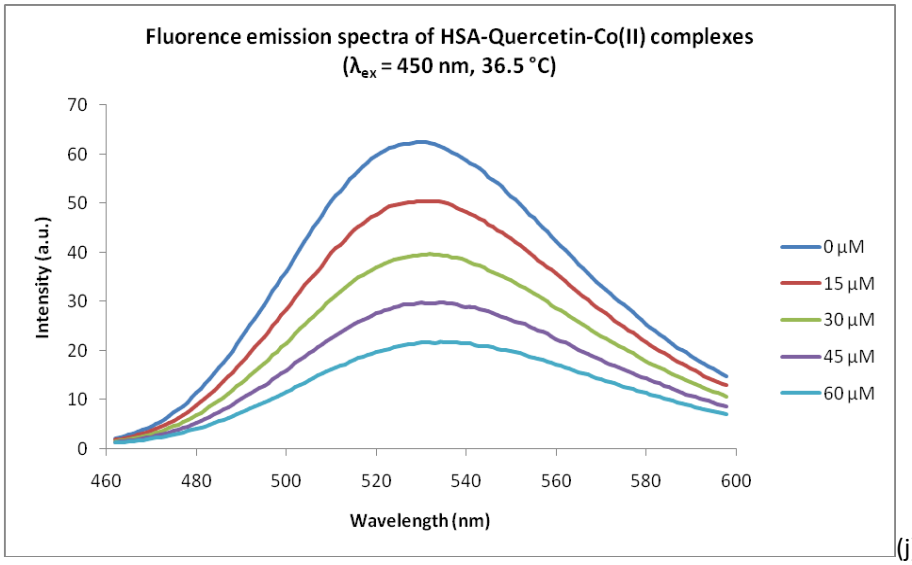

(j)

Figure 4: Fluorescence studies of HSA-quercetin-Co(II) complexes. All experiments were performed using a scan rate of 120 nm/min. (a) and (b) Excitation spectra of solutions containing 30 µM HSA, 15 µM quercetin,and varying amounts of Cd(II) in 50 mMTris-HCl buffer at temperatures of 30 and 36.5 °C, respectively. (c) and (d) Emission spectra of the same solutions in (a), using an excitation wavelength of 276 nm at temperatures of 30 and 36.5 °C, respectively. (e) and (f) Emission spectra of the same solutions in (a), using an excitation wavelength of 295 nm with range 305-400 nm at temperatures of 30 and 36.5 °C, respectively. (g) and (h) Emission spectra of the same solutions in (a), using an excitation wavelength of 295 nm with range 490-575 nm at temperatures of 30 and 36.5 °C, respectively. (i) and (j) Emission spectra of the same solutions in (a), using an excitation wavelength of 450 nm at temperatures of 30 and 36.5 °C, respectively.

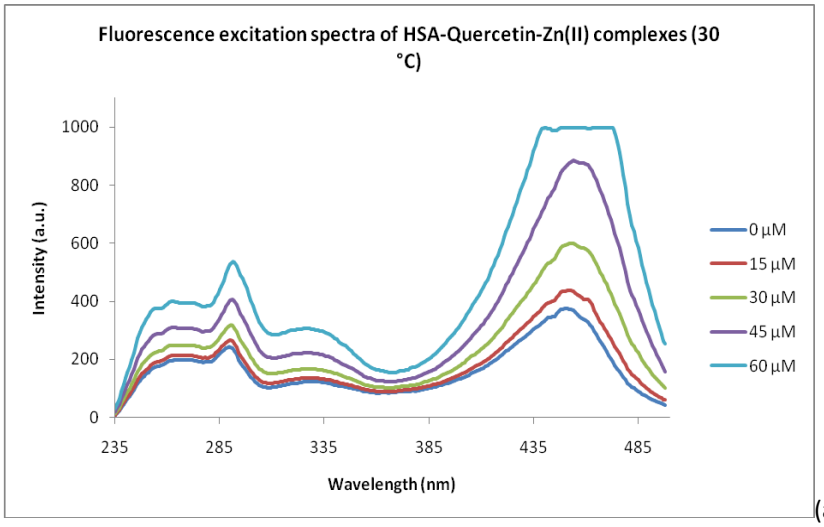

(a)

ISSN: 0975-8585

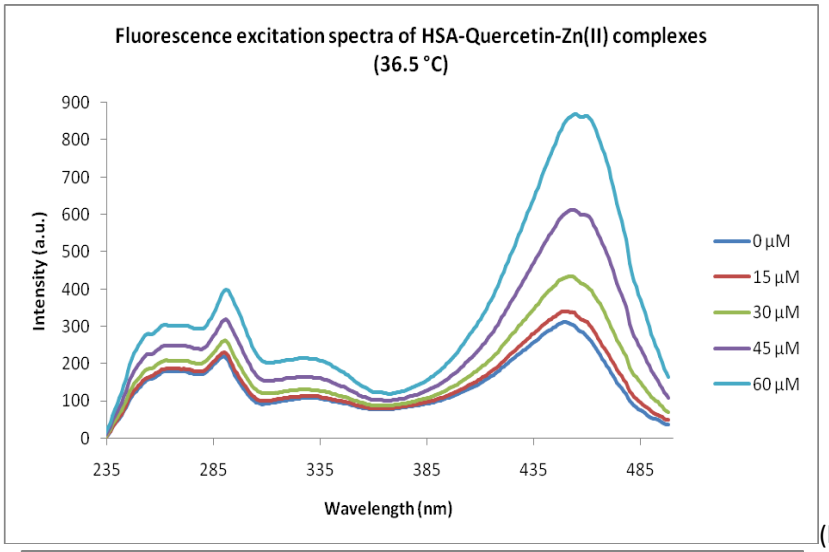

(b)

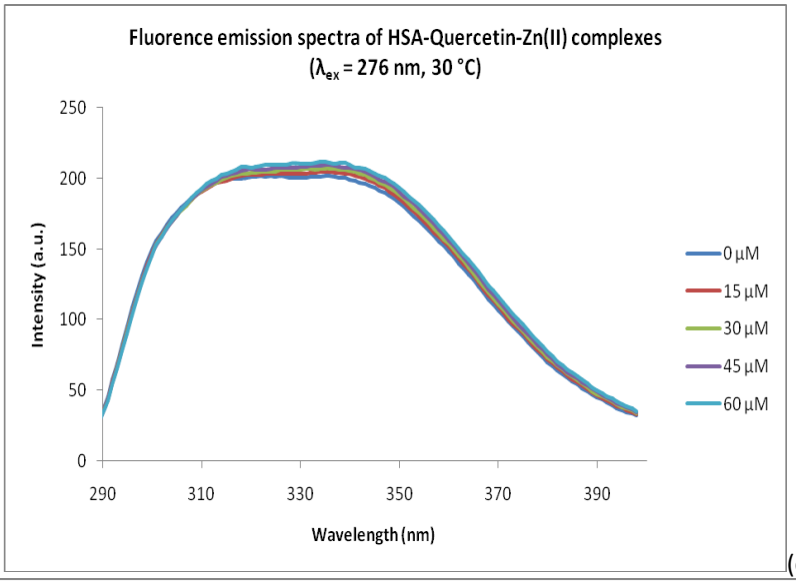

(c)

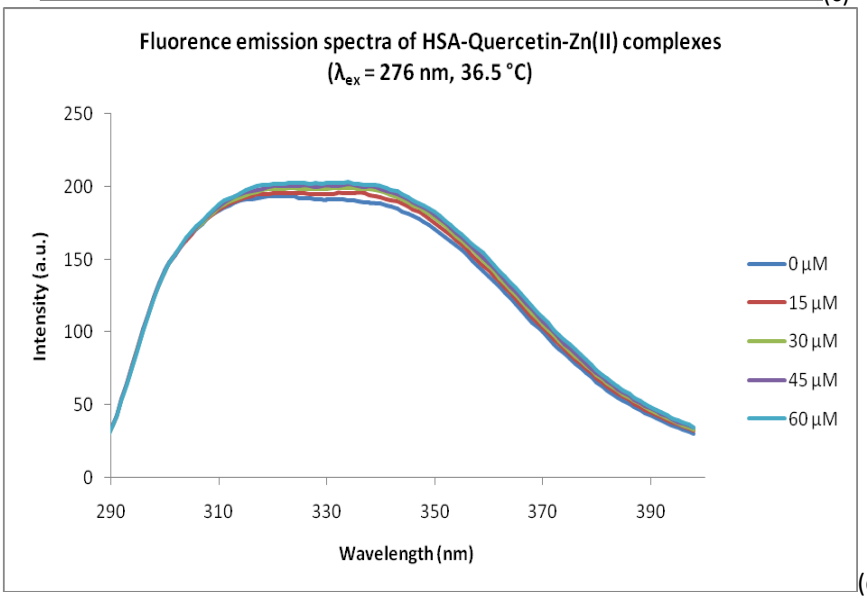

(d)

ISSN: 0975-8585

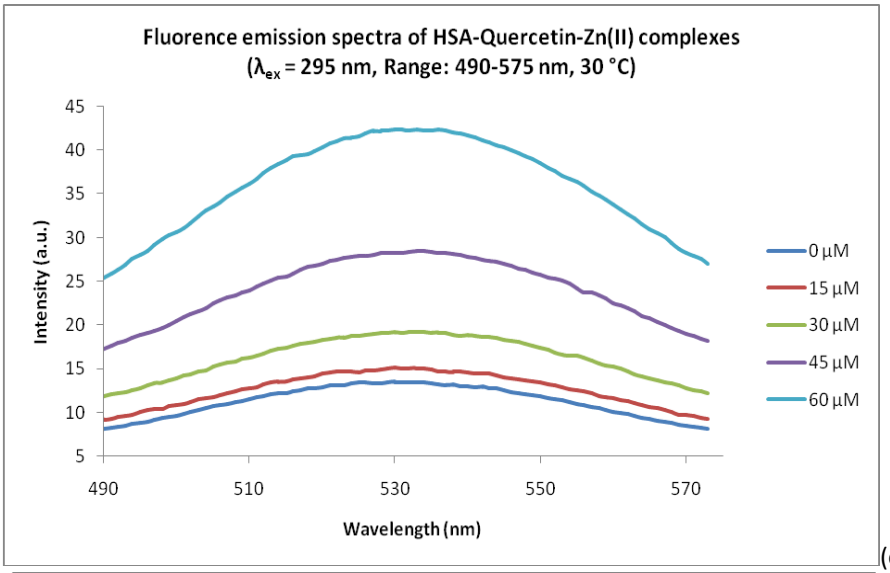

(e)

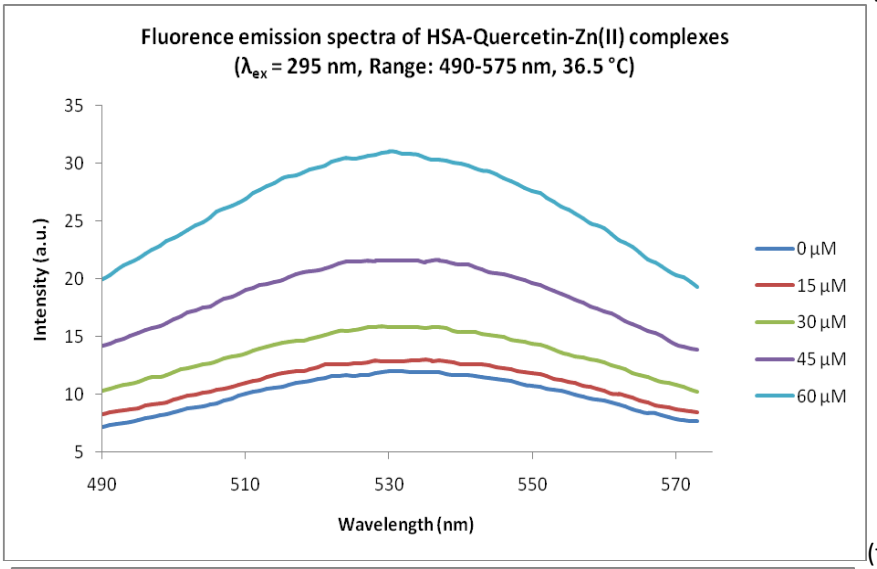

(f)

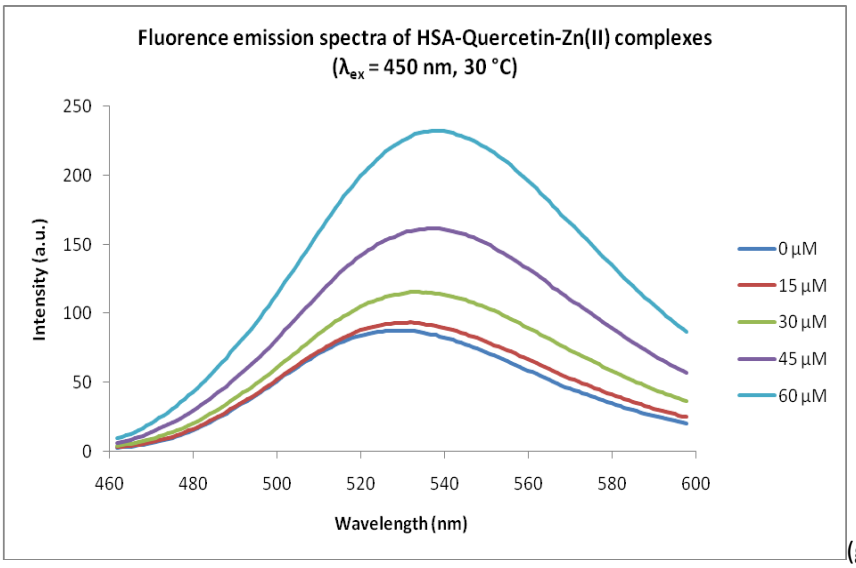

(g)

ISSN: 0975-8585

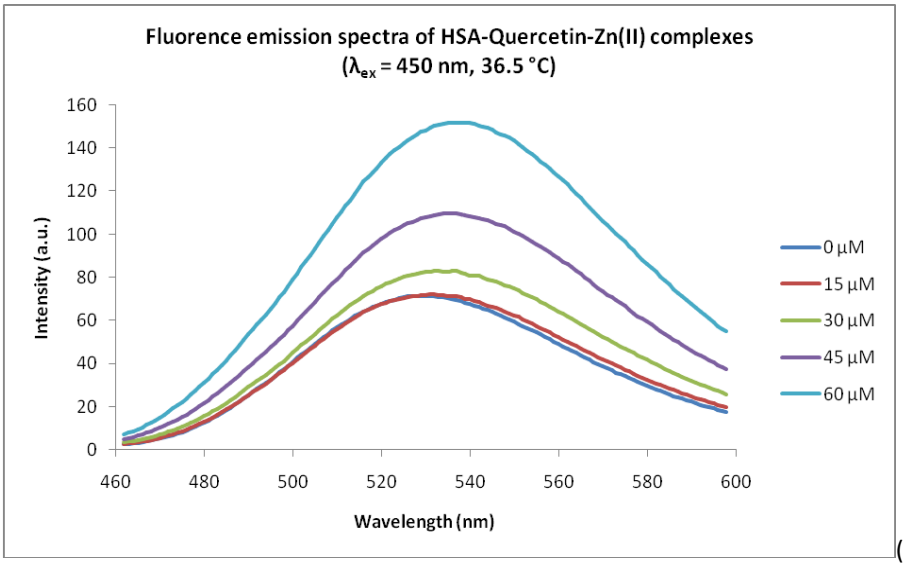

(h)

Figure 5: Fluorescence studies of HSA-quercetin-Zn(II) complexes. All experiments were performed using a scan rate of 120 nm/min. (a) and (b) Excitation spectra of solutions containing 30 µM HSA, 15 µM quercetin,and varying amounts of Cd(II) in 50 mMTris-HCl buffer at temperatures of 30 and 36.5 °C, respectively. (c) and (d) Emission spectra of the same solutions in (a), using an excitation wavelength of 276 nm at temperatures of 30 and 36.5 °C, respectively. (e) and (f) Emission spectra of the same solutions in (a), using an excitation wavelength of 295 nm at temperatures of 30 and 36.5 °C, respectively. (g) and (h) Emission spectra of the same solutions in (a), using an excitation wavelength of 450 nm at temperatures of 30 and 36.5 °C, respectively.

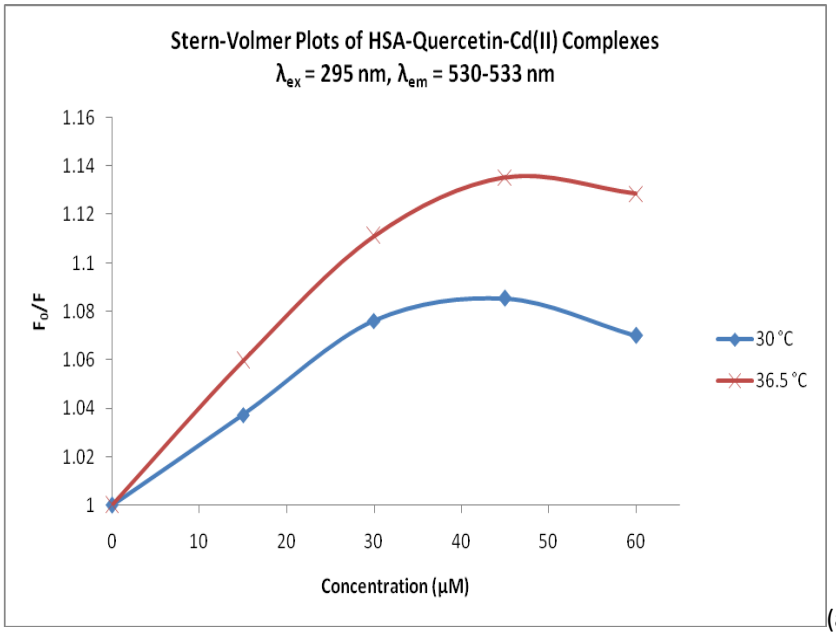

(a)

ISSN: 0975-8585

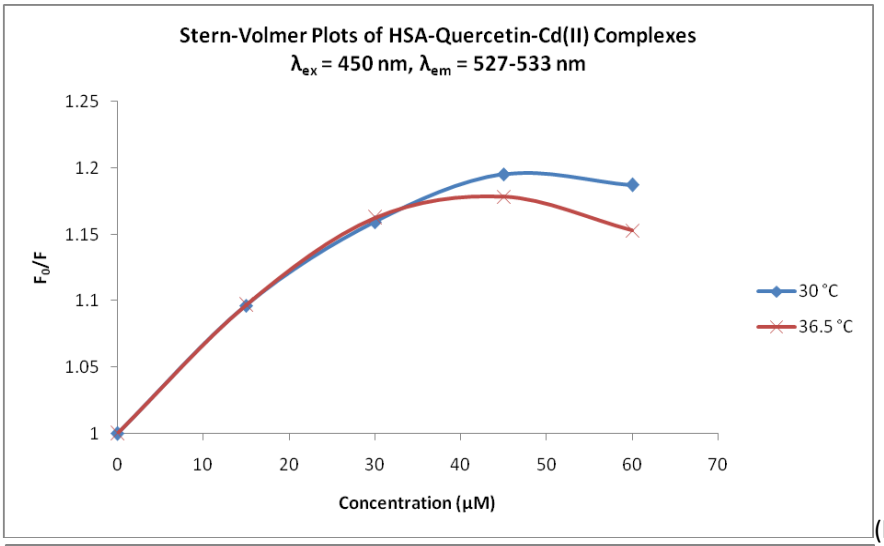

(b)

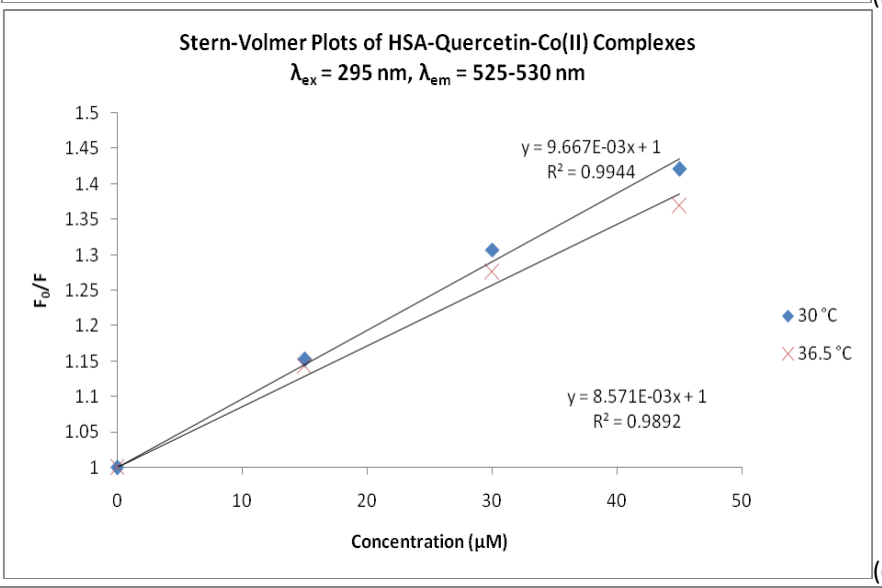

(c)

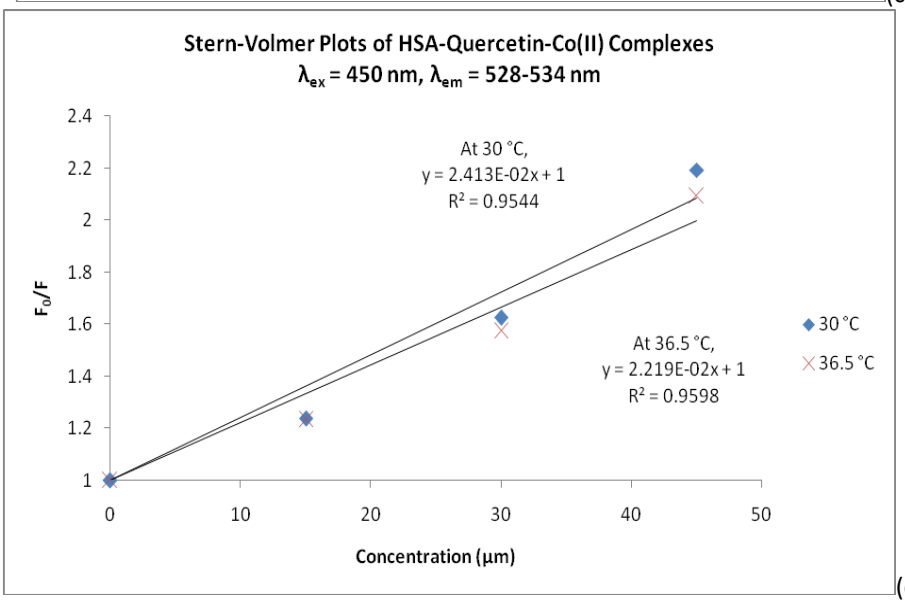

(d)

Figure 6: Stern-Volmer plots to determine the quenching mechanism(s) in HSA-quercetin-metal ion complexes.All emission spectra were recorded using solutions of 15 µM HSA, 15 µM quercetin and varying amounts of divalent metal ions, in 50 mMTris-HCl buffer, at temperatures of either 30 or 36.5°C (as specified). (a) Analysis for Cd(II) using an excitation wavelength of 295 nm and emission wavelengths

ISSN: 0975-8585

between 530-533 nm. (b) Analysis for Cd(II) using an excitation wavelength of 450 nm and emission wavelengths between 527-533 nm.(c) Analysis for Co(II) using an excitation wavelength of 295 nm and emission wavelengths between 525-530 nm. (d) Analysis for Co(II) using an excitation wavelength of 450 nm and emission wavelengths between 528-532 nm.

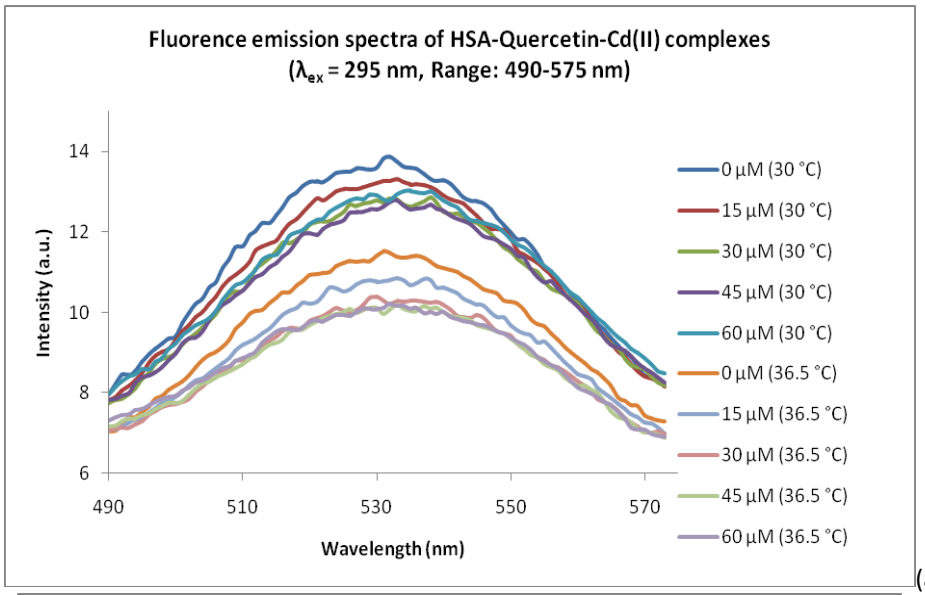

(a)

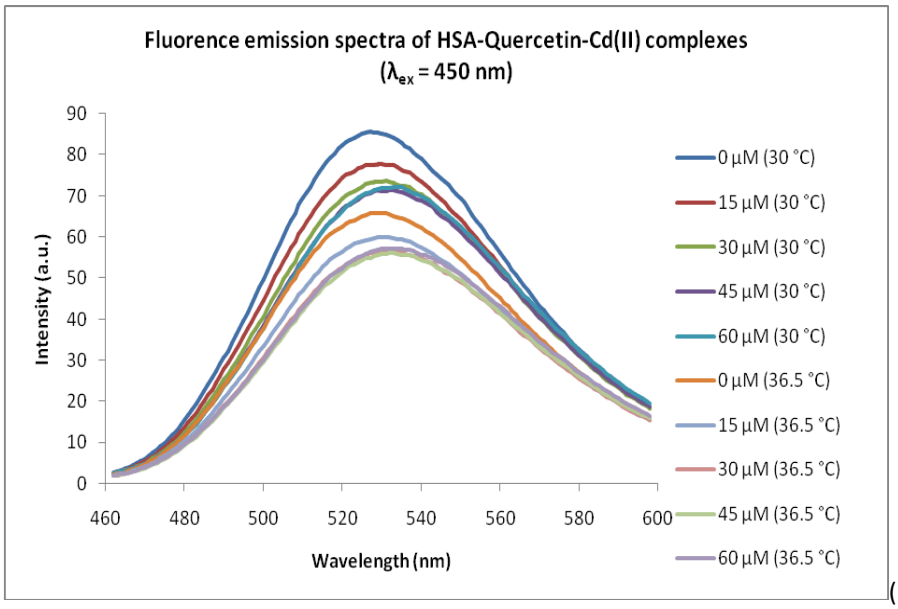

(b)

ISSN: 0975-8585

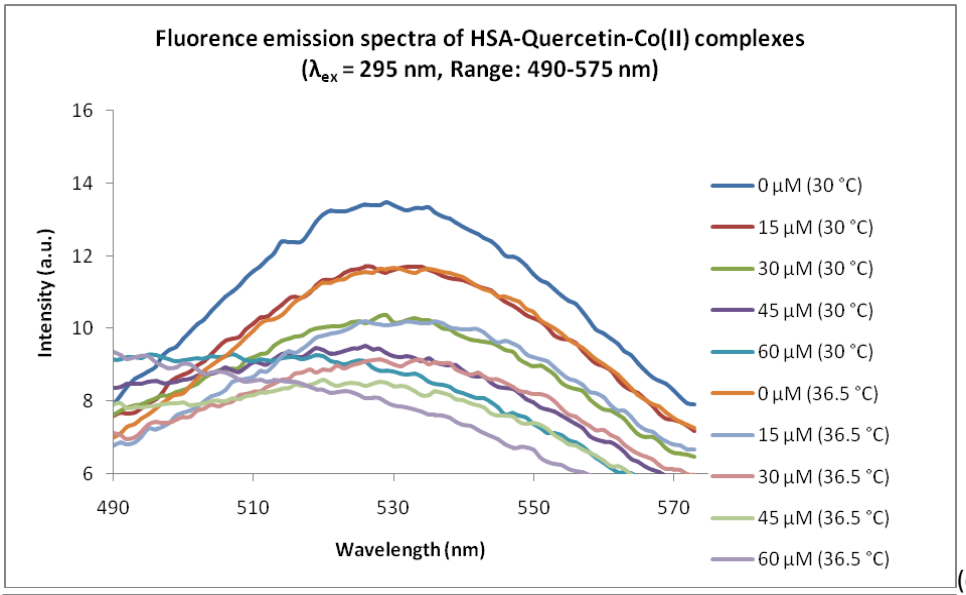

(c)

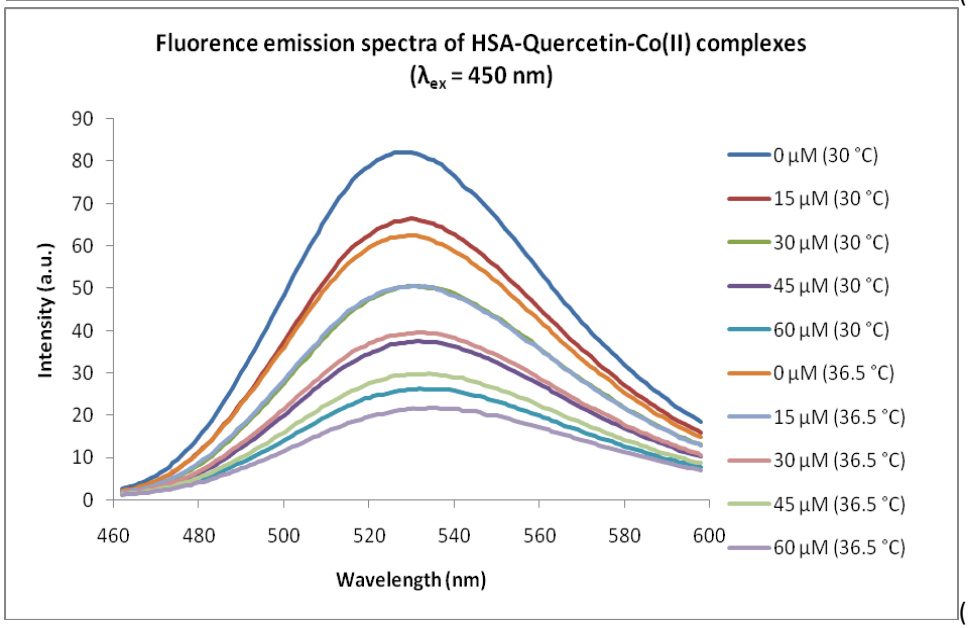

(d)

Figure 7: Quercetin fluorescence in HSA-quercetin-metal ion complexes. All emission spectra were recorded using solutions of 30 µM HSA, 15 µM quercetin and varying amounts of divalent metal ions, in 50 mMTris-HCl buffer, at temperatures of either 30 or 36.5°C (as specified), and a scan rate of 120 nm/min. (a) Emission spectra of Cd(II) complexes using an excitation wavelength of 295 nm. (b) Emission spectra of Cd(II) complexes using an excitation wavelength of 450 nm. (c) Emission spectra of Co(II) complexes using an excitation wavelength of 295 nm. (d) Emission spectra of Co(II) complexes using an excitation wavelength of 450 nm.

CONCLUSIONS

HSA-quercetin complexes in the presence of Cd(II), Zn(II), and Co(II) were studied using fluorescence spectroscopy. The effects solvents have on the intensity of fluorescence were studied before conducting experiments on the HSA-quercetin complex. It was noted that, as expected, there was a negligible effect of solvent on the intensity (data not shown). Additional experiments were done to determine whether any of the metal cations fluoresce in 50 mM Tris-HCl buffer. Neither Cd(II), Zn(II), nor Co(II) fluoresced in 50 mM Tris-HCl buffer. The next experiment studied the interaction of 30 µM HSA and 15 µM quercetin to determine fluorescence quenching and band shifts due to quercetin. Based on previous research and the HSA-quercetin experiment, the following table was made (Table 3):

ISSN: 0975-8585

Table 3: Excitation and emission wavelengths for various peak sources

λ_{ex} (nm)	λ_{em}^{*} (nm)	Peak Source
276	340	Tryptophan and tyrosine residues
295	343	Tryptophan-214
295	525	QC1 by fluorescence resonance transfer
380	525	QC1
450	525	QC2

*The emission peaks varied within a small range of wavelengths

Using these parameters, the effect a metal cation had on the two quercetin moieties was studied. Fluorescence quenching studies of the HSA-quercetin complex by Cd(II), Zn(II), and Co(II) were completed by interpreting fluorescence spectra and Stern-Volmer plots.

As the temperature increased, emission peaks were quenched in all emission spectra as shown in Tables4 –6. As stated earlier, only tryptophan-214 is able to be excited at 295 nm. A change by Cd(II) addition in a tryptophan emission was insignificant since the degree of change in intensity was small and could be attributed to noise. Therefore, Cd(II) does not affect tryptophan when HSA forms a complex structure with quercetin. However, Co(II) was able to quench tryptophan fluorescence.

Table 4: Summary of fluorescence emission spectra of the HSA-quercetin complex upon the addition of Cd(II)

Spectra Name	λ_{ex} (nm)	λ_{em}^{*} (nm)	Temp (°C)	Quencher Effect	Temperature Effect
$Em_{trp,tyr}$	276	335-337	30	Noise***	weak blue-shifted band**, quenches a peak
		320-325	36.5	enhances a peak**	
Em_{trp}	295	344-345	30	quenches a peak**	quenches a peak
		342-345	36.5	quenches a peak**	
$Em_{QC1,295}$		530-533	30	red-shifted band, quenches a peak	weak red-shifted band**, quenches a peak
		530-533	36.5	red-shifted band, quenches a peak	
$Em_{QC1,380}$	380	535-539	30	red-shifted band, quenches a peak	weak red-shifted band**, quenches a peak
		535-540	36.5	red-shifted band, quenches a peak	
Em_{QC2}	450	527-533	30	red-shifted band, quenches a peak	quenches a peak
		527-533	36.5	red-shifted band, quenches a peak	

*The emission peaks varied within a small range of wavelengths. **Change was small and can be considered negligible since it is possibly just noise. ***The change was observed without a distinct pattern.

Table 5: Summary of fluorescence emission spectra of the HSA-quercetin complex upon the addition of Zn(II)

Spectra Name	λ_{ex} (nm)	λ_{em}^{*} (nm)	Temp (°C)	Quencher Effect	Temperature Effect
$Em_{trp,tyr}$	276	334-336	30	enhances a peak**	weak blue-shifted band**, quenches a peak
		322-325	36.5	enhances a peak**	
Em_{trp}	295	344-346	30	quenches a peak**	quenches a peak
		343-345	36.5	enhances a peak**	
$Em_{QC1,295}$		530-536	30	enhances a peak	quenches a peak
		530-535	36.5	enhances a peak	
$Em_{QC1,380}$	380	538-541	30	enhances a peak	quenches a peak
		538-542	36.5	enhances a peak	
Em_{QC2}	450	528-539	30	red-shifted band, enhances a peak	blue-shifted band, quenches a peak
		528-537	36.5	red-shifted band, enhances a peak	

*The emission peaks varied within a small range of wavelengths. **Change was small and can be considered negligible since it is possibly just noise

ISSN: 0975-8585

Table 6: Summary of fluorescence emission spectra of the HSA-quercetin complex upon the addition of Co(II)

Spectra Name	λ_{ex} (nm)	λ_{em}* (nm)	Temp (°C)	Quencher Effect	Temperature Effect
$Em_{trp,tyr}$	276	334-336	30	enhances a peak**	weak blue-shifted band**,quenches a peak
		320-324	36.5	enhances a peak**	
Em_{trp}	295	343-344	30	quenches a peak	quenches a peak
		342-344	36.5	quenches a peak	
$Em_{QC1,295}$		525-529	30	quenches a peak	weak red-shifted band**, quenches a peak
		525-530	36.5	quenches a peak	
$Em_{QC1,380}$	380	538-539	30	quenches a peak	weak red-shifted band**, quenches a peak
		538-542	36.5	quenches a peak	
Em_{QC2}	450	528-532	30	red-shifted band, quenches a peak	quenches a peak
		530-534	36.5	red-shifted band, quenches a peak	

*The emission peaks varied within a small range of wavelengths. **Change was small and can be considered negligible since it is possibly just noise

When the HSA-quercetin complex is excited at 295 nm and 380 nm, emission peaks around 530 nm occur. Those peaks are from the same fluorophore, QC1. For Cd(II) and Co(II), $Em_{QC1,295}$ showed a weak red-shifted emission band when temperature increased. There is no band shift in the Em_{QC2} peak for Cd(II) and Co(II) when temperature increased. This confirms that QC1 and QC2 are two different moieties since temperature affects them in different ways. The addition of Cd(II) and Co(II) caused the Em_{QC2} peak to shift to longer wavelengths. This result confirms Kim's hypothesis that band shape of QC2 only shifts when tryptophan and tyrosine emission are quenched [4]. It also means that the weak quenching of the tryptophan peak at excitation of 295 nm when Cd(II) was added was a mix of noise and actual quenching. SV plots determined the quenching mechanism of QC1 and QC2 for Cd(II) and Co(II).The SV plots at 30 and 36.5 °C for quenching of the HSA-quercetin complex by Cd(II), Zn(II), and Co(II) are listed in Table 7. Only the SV relationships having high R^2 values for regression could be used to determine the specific quenching mechanism. A linear SV relationship was present in the quenching of QC1 by Co(II). Since the SV plot moves to the x-axis when temperature is increased, the quenching mechanism for QC1 by Co(II) was determined to be static quenching. Other SV plots including QC1 and QC2 quenching by Cd(II) , and QC2 quenching by Co(II) had R^2 values below 0.99. Thus, the quenching of those peaks was done with a mixture of static and collisional quenching. For QC1 and the addition of Cd(II), the dominant mechanism is collisional quenching. For QC2 and the addition of Cd(II), the dominant mechanism is collisional quenching for concentrations of 30 µM Cd(II) and static quenching for higher concentrations. The SV plots for Cd(II) are concave down, which indicates that the fluorophore is shielded when Cd(II) is added. This possibly occurs due to Cd(II)'s affinity to MBS and site B. Cd(II) has an equal affinity to MBS and site B (Table 1). The location of site B is not known. It is possible that binding to site B could cause a conformational change in the fluorophores. A fluorophore conformational change could be caused by binding to MBS.

Table 7: Summary of the SV plots of the HSA-quercetin complex upon the addition of Cd(II), Zn(II), or Co(II)

Quencher Type	Spectra Name	Temp (°C)	K_{SV} (10^3 L/mole)	R^2	Direction of the SV Plot Moving upon Increasing Temperature
Cd(II)	$Em_{QC1,295}$	30	N/A	N/A	y-axis
		36.5			
	Em_{QC2}	30			y-axis at concentrations 30 µM and lower; x-axis at higher concentrations
		36.5			
Zn(II)	$Em_{QC1,295}$	30	N/A	N/A	N/A
		36.5			
	Em_{QC2}	30			
		36.5			
Co(II)	$Em_{QC1,295}$	30	9.667	0.9944	x-axis
		36.5	8.571	0.9892	
	Em_{QC2}	30	24.13	0.9544	x-axis
		36.5	22.19	0.9598	

For QC1 and QC2 with the addition of Zn(II), no quenching occurs. In fact, the emission peaks increased. The most likely reason for this is Zn(II) strong affinity to MBS. Zn(II)'s dissociation constant at MBS is significantly lower than Cd(II)'s dissociation constant at the same site (Table 1). MBS is the dominant site for Zn(II) binding. MBS' proximity to tryptophan-214 possibly forces a conformational change. This change could lead to tryptophan-214 being further de-shielded and thus a higher intensity. For QC2 with the addition of Co(II), the dominant mechanism is static quenching since the SV plot moves toward the x-axis when temperature increased.

There is a possible connection between magnitude of the quenching by a metal ion and its affinity to bind to HSA. As shown in Figures 7a and 7b, the quenching of QC1 and QC2 by addition of 15 µM Cd(II) is less than the quenching of QC1 and QC2 by an increase of temperature. Thus temperature is a stronger quencher. As shown in Figure 7c and 7d, the quenching of QC1 and QC2 by addition of 15 µM Co(II) is approximately the same as the quenching of QC1 and QC2 by increase of temperature. These results can be explained by the dissociation constants. Cd(II) binds tighter to site B than Co(II) does.

In summary, two fluorophores from the binding of HSA and quercetin are quenched by Cd(II) and Co(II). The quenching was attributed to both static and collisional quenching. The band shape of QC1 was sensitive to the nature of the quencher and the temperature. The band shape of QC2 only shifted if tryptophan and tyrosine emission are quenched. These results confirm Kim's research [4]. Zn(II) enhanced the intensities of the two fluorophores. Higher binding affinities to NTS and site B lead to smaller quencher effects. High binding affinity to MBS leads to enhancement of the intensities of the two fluorophores.

ACKNOWLEDGMENTS

We would like to thankPatrick Chiu, Victoria Heinz, Liz Leon, and Dr. Chin Lin for their help with this project.

REFERENCES

[1] He XM, Carter DC. Nature1992; 358(6383): 209-215.
[2] Fasano M, Curry S, Terreno E, Galliano M, Fanali G, Narciso P, Notari S, Ascenzi P. International Union of Biochemistry and Molecular Biology: Life2005;57(12): 787-796.
[3] Sudlow G, Birkett DJ, Wade DN. Molecular Pharmacology 1976; 12(6): 1052-1061.
[4] Kim C, Savizky RM. Research Journal of Pharmaceutical, Biological and Chemical Sciences 2013; 4(2): 765-795.
[5] Sadler PJ, Viles JH. Inorganic Chemistry 1996; 35(15): 4490-4496.
[6] Bal W, Sokołowska M, Kurowska E, Faller P. Biochimica Et Biophysica Acta (BBA) - General Subjects2013; 1830(12): 5444-5455.
[7] Dantuluri M, Gunnarsson GT, Riaz M, Nguyen H, Desai UR. Analytical Biochemistry 2005; 336(2): 316-322.
[8] Galati G, O'brien PJ. Free Radical Biology and Medicine2004; 37(3): 287-303.
[9] Formica JV, Regelson W. Food and Chemical Toxicology 1995; 33(12): 1061-1080.
[10] Torreggian A,Tamba M, Trinchero A, Bonora S.Journal of Molecular Structure 2005; 744-747: 759-766.
[11] Dufour C, Dangles O. Biochimica Et Biophysica Acta (BBA) - General Subjects 2005; 1721(1-3): 164-173.
[12] Ravichandran R, Rajendran M, Devapiriam D. Food Chemistry2014; 146: 472-478.
[13] Sengupta B, Sengupta PK. Biochemical and Biophysical Research Communications 2002; 299(3): 400-403.
[14] Zsila F, Bikádi Z, Simonyi M. Biochemical Pharmacology2003; 65(3): 447-456.
[15] Lakowicz JR. Principles of Fluorescence Spectroscopy. Springer New York, 2006; 3-283.
[16] Mátyus L, Szöllősi J,Jenei A. Journal of Photochemistry and Photobiology B: Biology2006; 83(3): 223-236.
[17] Lehrer S. Biochemistry 1971; 10(17): 3254-3263.